Failure strength of brittle materials containing nanovoids

Mariella Ippolito,[1,2] Alessandro Mattoni,[2] Nicola Pugno,[3] and Luciano Colombo[1,2,*]
[1]*Department of Physics, University of Cagliari, Cittadella Universitaria, I-09042 Monserrato, Cagliari, Italy*
[2]*Sardinian Laboratory for Computational Materials Science (SLACS, CNR-INFM), c/o Department of Physics, University of Cagliari, Cittadella Universitaria, I-09042 Monserrato (Ca), Italy*
[3]*Department of Structural Engineering and Geotechnics, Politecnico di Torino, I-10138 Torino, Italy*
(Received 4 August 2006; revised manuscript received 30 March 2007; published 15 June 2007)

By means of atomistic simulations, we investigate the failure strength in plane strain conditions of a brittle solid containing nanosized stress concentrators, i.e., a straight crack, a cylindrical hole, or a spherical hole. We find that the failure strength of the defected solid strongly depends on the defect size, in contrast with the predictions of standard elasticity theory. A high strength reduction due to voids as large as few atoms is observed. Such results have been included in two analytical failure criteria, namely, the average stress criterion and the point stress criterion. Both models introduce a length scale typical of the system, tailored at describing the process zone near the nanovoids. We provide a numerical estimate for this length scale, which is found to be specific for any defect, and we reconcile atomistic results to continuum into a coherent picture.

DOI: 10.1103/PhysRevB.75.224110 PACS number(s): 62.25.+g, 62.20.Mk, 81.40.Np

I. INTRODUCTION

Defects such as cracks and voids affect the mechanical behavior of brittle solids since they modify the overall strength of the material. Sometimes such defects are unavoidable because they form during materials synthesis and processing such as, e.g., ceramic sintering. On the other side, voids may be introduced into the material by design in order to obtain specific properties. This is the case of porous materials where pores at a suitable concentration are used to control the thermal or acoustic isolation, the impact energy absorption, and many other properties.[1] In any case, such inhomogeneities are of great relevance on the mechanical response of the system, since they enhance the local stress and they possibly may initiate failure. In addition, as the technological demand for extremely high strength materials increases (as well as the development of nanoscale devices or machines), defects as small as a few nanometers cannot be neglected. As an example, it has been recently found that even one- or two-atom vacancy defect can reduce the failure strength of carbon nanotubes by an amount of 26%.[2,3] We will show that sizable strength reduction due to voids as large as few atoms are observed in bulk β-SiC as well.

The strength of materials containing cracks and voids is traditionally described according to *stress intensification* or *stress concentration* arguments, respectively.[4,5] The need of different approaches is motivated, according to linear elastic fracture mechanics (LEFM), by the mathematical divergence of the stress field near the crack tip. Following LEFM, loading produces a $1/\sqrt{x}$ singularity at the crack tip (where x is the distance from the crack tip along the plane of the crack) and a critical stress equal to zero is expected. As a consequence, a straightforward prediction of failure stress as uniquely based on local stress criteria cannot be applied. The critical stress of the cracked body is therefore calculated by analyzing the stress singularity at the crack tip: the failure takes place when the stress intensity factor K is equal to the material fracture toughness K_c.[6,7] This criterion relies on the energy balance of the Griffith theory.[8] In contrast, elasticity theory predicts that the failure from a void (as it is the case of cylindrical or spherical holes) takes place when the maximum local stress equals the ideal material strength σ_{th}.[5] Both alternative continuum approaches (for cracks and voids) are based on linear elasticity and they unlikely work at the nanoscale. Their possible weaknesses could, in principle, be due to the failure of at least one of the three underlying (constitutive) hypotheses they rely on: either continuum mechanics, elasticity, or linearity.

In order to improve classical continuum models, modern theories of fracture are generally formulated so as to incorporate into their formalism a suitable material length scale λ: this key quantity is aimed at describing a process zone close to the crack tip where at least one of the above constitutive hypotheses fails. The characteristic length scale is typically given by

$$\lambda \sim \frac{2K_c^2}{\pi\sigma_{th}^2}. \tag{1}$$

The interpretation of the length λ is not unique and it could be related to the existence of either a plastic zone (i.e., the mechanical response is beyond pure elasticity), a cohesive zone (linearity is lost), or a discrete unit for crack advancement (continuum hypothesis is no longer applicable).

In the framework of brittle fracture formalism, the characteristic length λ has been incorporated in four different models. The point stress criterion[9,10] (PSC) assumes that the failure occurs if the stress becomes equal to σ_{th} at a suitable distance l from the notch, corresponding to $l \sim \lambda/4$. An alternative approach is the average stress criterion[9,10] (ASC) according to which the failure occurs if the mean value of the stress along a line (or a surface, or a volume) starting at the notch root is equal to σ_{th}; the length l of such a line is in this case as large as λ. Furthermore, the equivalent linear elastic fracture mechanics (equivalent LEFM)[4] assumes the existence of a crack at the root of the notch (i.e., the effective crack length is longer than its original size): the failure is predicted to occur when this effective crack reaches the criti-

cal stress intensity factor (or energy release rate). The size l of the effective correction to the crack length is $\lambda/2$. Finally, a more recent approach is represented by the quantized fracture mechanics (QFM) (Ref. 11): the condition for failure is here derived by using a discrete counterpart of the Griffith approach and it is still based on an energy balance criterion. The failure is predicted when the root mean square of the stress intensity factor along a finite length—named *fracture quantum*—is equal to K_c (or equivalently when the mean energy release rate reaches a critical value). In this case, the fracture quantum l is equal to λ. Note that other discretized failure criteria in static brittle fracture, as well as in dynamic and fatigue fracture, have been recently introduced.[12]

Whereas ASC and QFM are physically sound and they interpret the length λ of the process zone as the discrete unit for crack advancement, PSC and equivalent LEFM do not provide a similar robust interpretation of such a key quantity. However, we point out that none of the above theories is able to quantify the actual value of the length scale l: typically, it must be estimated by fitting from experiments.

In this work, we use atomistic simulations to investigate the fundamental issues underlying the failure criteria of a material containing nanovoids. We compare PSC and ASC models with the calculated failure strength in nanodefected crystalline β-SiC and we provide an estimate for the characteristic length scale (i.e., process zone size) in the cases of cracks and both cylindrical and spherical holes. In our work, atomistic simulations are viewed at as a sort of "*ab initio* mechanical theory," which is able to discriminate among different fracture models since it is not based on a constitutive mechanical behavior guessed *a priori*.

The paper is organized as follows. In Sec. II, we summarize the classical continuum results for the stress field of a system containing a crack, a cylindrical hole, or a spherical hole, and we calculate the corresponding failure strength according to the ASC and PSC models. In Sec. III, we describe the geometry and the computational framework of the present atomistic simulations. In Sec. IV, the atomistic results are extensively compared with the elasticity theory and with the ASC and PSC predictions and some conclusions are consistently drawn.

II. ANALYTICAL MODELS

We focus our analysis on a homogeneous system under uniaxial load σ_A and containing at its center a straight crack, a cylindrical hole, or a spherical void. The geometry of the system is reported in Fig. 1.

In the case of uniaxially loaded system, two lateral border conditions are usually adopted in continuum mechanics, namely, plane strain or plane stress.[6] In the first case, the strain in the plane x-y orthogonal to the applied load is set to zero (with reference to Fig. 1, this is equivalent to setting $\varepsilon_{xx}=\varepsilon_{yy}=0$). At variance, in plane stress border condition the stress in the x-y plane is fixed to zero (with reference to Fig. 1, this is equivalent to setting $\sigma_{xx}=\sigma_{yy}=0$).

The actual effect of the above border conditions on the failure strength σ_f depends on both the Young modulus E and the Poisson ratio ν of the material. In general, within LEFM, it is proved that[6]

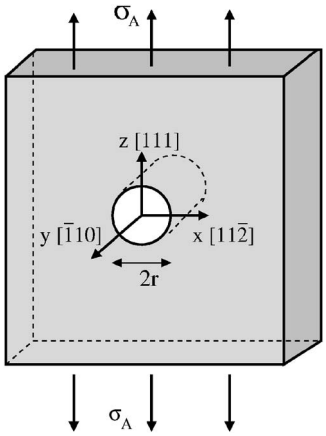

FIG. 1. Geometry of a system containing a cylindrical hole and strained along the z direction. The alignment of the crystallographic axes is reported. A similar geometry is assumed for a straight crack and a spherical hole.

$$\sigma_f = \sqrt{\frac{2\gamma E'}{\pi r}} \tag{2}$$

for a system containing a crack of semilength r. γ is the surface energy. The actual value of E' is, respectively, $E'=E$ for plane stress and $E'=E/(1-\nu^2)$ for plane strain border conditions. Thus, the difference of the failure strength predicted in the two cases is expected to be small for materials characterized by a small Poisson ratio. This is, in fact, the case of the present investigation focused on β-SiC, where $\nu \simeq 0.05$ for the selected crystallographic alignment.[20]

In the case of a crack of semilength r, the z component of the stress along the x axis is[6,7]

$$\sigma_{zz}(x) = \sigma_A \frac{x}{\sqrt{x^2 - r^2}}. \tag{3}$$

Close to the crack tip (i.e., when $x \to r$), the stress diverges and therefore the failure condition cannot be straightforwardly obtained by a criterion based on such a quantity (otherwise we should conclude that the failure occurs at vanishing load: this is the well-known paradox of the LEFM).

According to elasticity theory,[5] the stress $\sigma_{zz}(x)$ near a cylindrical hole of radius r is given by

$$\sigma_{zz}(x) = \frac{\sigma_A}{2}\left(2 + \frac{r^2}{x^2} + 3\frac{r^4}{x^4}\right), \tag{4}$$

while for a spherical hole, we have

$$\sigma_{zz}(x) = \frac{\sigma_A}{2}\left(2 + \frac{4}{7}\frac{r^3}{x^3} + \frac{9}{7}\frac{r^5}{x^5}\right). \tag{5}$$

Both cases are obtained in the limit of vanishing Poisson ratio ($\nu \sim 0$). However, we verified that by releasing such an approximation the results were practically unchanged. In the limit $x \to r$, Eqs. (4) and (5) give $\sigma_{zz}(r)/\sigma_A \sim 3$ and 2, respectively. In both cases, the stress concentration at the hole border ($x=r$) does not depend on the hole radius. In addition, we remark that the stress concentration at the hole boundary

strictly depends on the hole size[13–16]; thus, the applicability of elasticity theory is restricted to the case of very large radii.

A unified treatment for sharp (i.e., cracks) and blunt (i.e., holes) stress concentrators—valid for any defect size and shape—is not only worthy but also needed. To this aim, Whitney and Nuismer[9,10] developed two alternative models based on the nonlocal stress concept, namely, ASC and PSC. According to ASC (which is based on Novozhilov stress theory[17]), the failure occurs when the average value of $\sigma_{zz}(x)$ over the length l reaches the ideal tensile strength σ_{th},

$$\frac{1}{l}\int_{r}^{r+l}\sigma_{zz}(x)=\sigma_{th}. \tag{6}$$

By combining Eqs. (6) and (3) and by imposing the critical condition $\sigma_A=\sigma_f$, the failure strength in the case of a straight crack is

$$\frac{\sigma_f}{\sigma_{th}}=\frac{1}{\sqrt{1+2c/l}}. \tag{7}$$

Similarly, by combining Eqs. (4) and (6), we obtain for a cylindrical hole

$$\frac{\sigma_f}{\sigma_{th}}=\frac{2}{2-\frac{r}{l}\left(\frac{1}{l/r+1}-1\right)-\frac{r}{l}\left(\frac{1}{(l/r+1)^3}-1\right)}. \tag{8}$$

Finally, for the spherical hole case, by combining Eqs. (5) and (6) we get

$$\frac{\sigma_f}{\sigma_{th}}=\frac{2}{2-\frac{2}{7}\frac{r}{l}\left(\frac{1}{(l/r+1)^2}-1\right)-\frac{9}{28}\frac{r}{l}\left(\frac{1}{(l/r+1)^4}-1\right)}. \tag{9}$$

As for PSC, the failure occurs when the stress $\sigma_{zz}(x)$ at a small fixed distance l from the crack tip (or from the hole boundary) equals the tensile strength of the material,

$$\sigma_{zz}(x)|_{x=r+l}=\sigma_{th}. \tag{10}$$

Through Eqs. (10) and (3), and by imposing the critical condition, we obtain

$$\frac{\sigma_f}{\sigma_{th}}=\frac{1}{\sqrt{1-\frac{1}{(l/r+1)^2}}} \tag{11}$$

for the crack case. Finally, by substituting Eq. (4) or (5) into Eq. (10), we get the PSC estimation for the failure strength in the case of a cylindrical hole,

$$\frac{\sigma_f}{\sigma_{th}}=\frac{2}{2+\frac{1}{(l/r+1)^2}+3\frac{1}{(l/r+1)^4}}, \tag{12}$$

or a spherical hole,

$$\frac{\sigma_f}{\sigma_{th}}=\frac{2}{2+\frac{4}{7}\frac{1}{(l/r+1)^3}+\frac{9}{7}\frac{1}{(l/r+1)^5}}, \tag{13}$$

respectively.

It should be understood that, for sake of simplicity, Eqs. (6)–(13) are written using the same symbol l. Nevertheless, as already commented, such a quantity assumes a different value in the ASC and PSC models.

III. ATOMISTIC SIMULATIONS

A. Geometry of the simulation cell and border conditions

In order to perform atomistic simulations on a system corresponding to the same geometry of Fig. 1, we adopted a simulation cell containing a β-SiC monocrystal under tensile load, embedding either a straight crack, a cylindrical hole, or a spherical hole. We then evaluated the failure strength of the defected β-SiC specimen as a function of the defect size and shape.

In order to implement the above protocol, the following numerical procedure has been adopted. As for the simulation cell, the x, y, and z axes were aligned along $[11\bar{2}]$, $[\bar{1}10]$, and $[111]$ orthogonal crystallographic directions, respectively. In the x-y plane, the simulation cell was kept fixed both in size and shape, and periodically repeated. In this plane, the lattice parameter was the equilibrium one for β-SiC, corresponding to 4.318 Å. A tensile load σ_A was applied along the z direction according to the constant traction method:[18] periodic boundary conditions were removed along the z direction and the resulting surfaces [in our case one top silicon and one bottom carbon (111) shuffle planes] were loaded by a constant traction mimicking the embedding into an infinite bulk at the same strain condition. As for the internal degrees of freedom (i.e., atomic positions), throughout the simulation they were completely free to relax in all directions.

Such a protocol of simulation does correspond to the plane strain border condition of continuum. The lateral stress (i.e., the σ_{xx} and σ_{yy} components) is computed to be small with respect to the z component of the stress, as expected from the small Poisson ratio of β-SiC. For example, for an ideal (i.e., not defected) sample we found that, close to the critical strain ($\varepsilon_{zz}\lesssim 20\%$, see Sec. IV), the ratio σ_{xx}/σ_{zz} is as small as $\simeq 4\%$. The same result holds for the σ_{yy} component as well; this is due to the in-plane symmetry. This suggests that the border conditions do not affect sizably the present physical picture. A further validation of this conclusion is discussed in the next section, where some calculations in plane stress condition are shown.

The crack was obtained by cutting a given number n of interatomic bonds across a segment of the central (111) plane in the strained simulation cell. Such a crack alignment is the most likely to occur since the (111) shuffle plane has the lowest surface energy for β-SiC. We point out that because of the very discrete nature of the lattice, there is an arbitrariness as large as c_0 in defining the size of the crack, where $c_0=2.644$ Å is the interbond distance along the x direction. This amounts to stating that the crack length $2r$ lies within

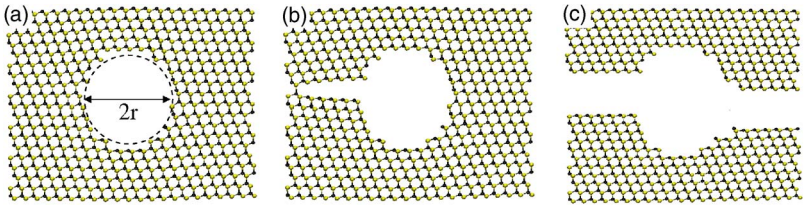

FIG. 2. (Color online) Atomic-scale view of the system under remote stress σ_A, containing a cylindrical hole. (a) $\sigma_A \ll \sigma_f$; (b) $\sigma_A \geqslant \sigma_f$, corresponding to fracture initiation; (c) complete failure. Note that there is an intrinsic uncertainty in the definition of the hole radius, as due to the atomic-scale surface morphology.

the range $c_0(n-1)$ and $c_0(n+1)$. We conventionally choose as crack length the average value $c_0 n$. We observe that when $\sigma_A < \sigma_f$, the initial cut relaxes to an elliptical Griffith-like hole. The length of the final defect turns out to decrease by a small amount ($\Delta c < c_0/8$) with respect to the initial crack, as a result of the atomic displacements due to the applied load.

The cylindrical and the spherical holes were in turn obtained by removing N_h atoms in a selected region of radius r at the center of the simulation cell. As far as concerns the hole size, it is defined to be $r+\delta r$, where δr is the maximum variation of the radius that does not modify the number N_h of removed atoms (we remark $\delta r \ll c_0$). The cylindrical voids were oriented along the y axis, perpendicular to the applied stress. We observe that a simulated hole of a given size can have a different surface structure depending on its position in the lattice. This is shown in Fig. 2, panel (a).

In the case of the straight crack, we considered the semilength r to vary in the range $c_0 < r < 25c_0$. As for the cylindrical hole, we varied the radius in the range 1.3 Å $< r <$ 40 Å. The smallest radius corresponds to the removal of a single row of silicon or carbon atoms. Finally, the radius of the spherical hole was 1.3 Å $< r <$ 20 Å, the smallest value corresponding to a single atom vacancy.

We used a simulation cell with dimensions $L_x = L_z = L$ and $L_y \ll L$ (typically $L_y \simeq 12$ Å) for cracks and cylindrical voids, while we used a cubic shape $L_x = L_z = L_y = L$ for spherical holes. In order to avoid finite-size effects, we set in any case $L/r > 10$. The resulting number of atoms ranged from 30 000 up to 250 000 for straight cracks and cylindrical voids, while up to 800 000 particles have been used for spherical holes. We verified that for larger size of the simulation cell ($L/r > 30$), the atomistic results were unchanged, thus proving that no size effects are expected in the present investigation.

B. Managing atom degrees of freedom

Interatomic forces were calculated according to the environment dependent Tersoff potential.[19] We have extensively proved its reliability for brittle fracture problems in β-SiC under many different conditions,[20–22] provided that some optimization of the cutoff function is developed.[25] The stress fields were calculated after the relaxation of the atomic forces based on the two-step damped dynamics (DD) method: (i) the atomic positions and velocities are firstly aged over the time interval ($t \rightarrow t+\delta t$) by ordinary finite-difference algorithms and then (ii) the atomic component α of velocity vectors $\mathbf{v}_i$ is set to zero for those atoms i that satisfy the condition

$$F_i^\alpha v_i^\alpha \leqslant 0. \tag{14}$$

The key idea of the DD method is that an atom is allowed to accelerate toward a minimum of configurational energy, while it is stopped when it attempts to escape from such a minimum-energy basin. The DD algorithm is iterated until the maximum atomic force is smaller than a suitable threshold; we evaluated that the system was fully relaxed for atomic forces below 10^{-4} eV/Å.

C. Atomic level stress tensor

The stress tensor $\Sigma_{\alpha\beta}$ of a system is, in principle, defined as[23]

$$\Sigma_{\alpha\beta} = \frac{1}{V}\frac{\partial U}{\partial \epsilon_{\alpha\beta}}, \tag{15}$$

where V is the system volume, U is the internal energy, and $\epsilon_{\alpha\beta}$ is the strain tensor for the Cartesian coordinates α and β. In Eq. (15), the internal energy U of the system can be written as the sum of single-site energies u_i, thus obtaining

$$\Sigma_{\alpha\beta} = \frac{1}{N}\sum_i \left(\frac{V}{N}\right)^{-1} \frac{\partial u_i}{\partial \epsilon_{\alpha\beta}} = \frac{1}{N\omega}\sum_i s_{\alpha\beta,i}, \tag{16}$$

where we indicate $\partial u_i/\partial \epsilon_{\alpha\beta} = s_{\alpha\beta,i}$ and we attribute to any atom the same volume $\omega = V/N$. Such an attribution is, in principle, correct for homogeneous systems only; nonetheless, we proved[24] that this is a quantitatively good approximation also for the present investigation where cracks and voids are present. For any pair i-j of interacting atoms, we calculated the average atomic stress $\sigma_{\alpha\beta}(x) = \frac{1}{2}(s_{\alpha\beta,i} + s_{\alpha\beta,j})$ and we attributed such a stress value to the average atomic position x of the selected i-j atom pair.

IV. RESULTS

The ideal strength of β-SiC was calculated by simulating a perfect bulk loaded along the [111] crystallographic axis up to the failure: the calculated critical strain and stress are $\varepsilon_{zz} \simeq 0.20$ and $\sigma_{th} = 58 \pm 1$ GPa, respectively. This value of σ_{th} is found to be about $E/10$, where the Young modulus was estimated to be $E = 556 \pm 1$ GPa. This result is in a qualitatively agreement with a standard ansatz of continuum mechanics.[6] The present values for the failure strength and the Young

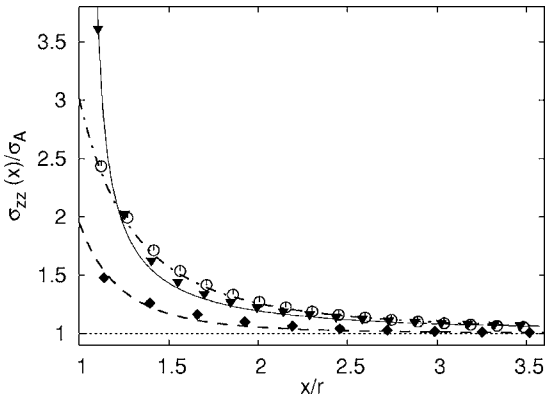

FIG. 3. Stress enhancement in front of a straight crack (full line), a cylindrical hole (dot-dashed line), and a spherical hole (dashed line) of dimension $r=1.8$ nm, $r=1.8$ nm, and $r=2.0$ nm, respectively. Symbols represent the atomistic data.

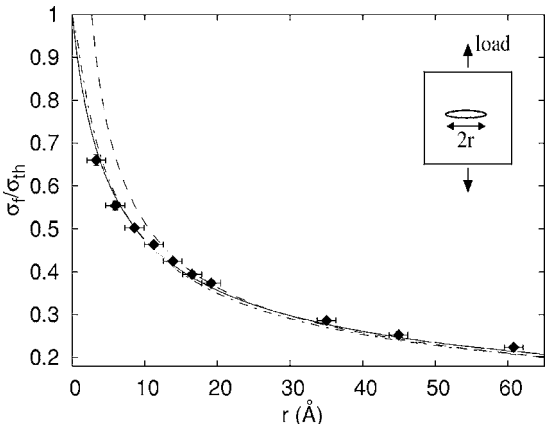

FIG. 4. Failure strength of a system containing a crack of semilength r. Black symbols represent the atomistic data (the horizontal error bars refer to the uncertainty in the definition of the crack length, as due to the atomic-scale crack-tip structure). The full and the dot-dashed line represent ASC and PSC data, respectively. The dashed line corresponds to the classical Griffith theory.

modulus are also close to density-functional theory results:[26] $\sigma_{th}\simeq 50.4$ GaP and $E\simeq 558$ GPa.

By using the calculated critical strength, it is possible to evaluate the length λ of the process zone according to Eq. (1). The fracture toughness K_c is calculated as $K_c=\sqrt{2\gamma E}$, where γ is the surface energy of the (111) shuffle plane.[6] We get $\lambda\simeq 5.4$ Å: the size of the process zone turns out to be as small as few lattice spacings so, as expected, it is relevant only at the nanoscale. We then calculated the stress enhancement $\sigma_{zz}(x)/\sigma_A$ induced by the three different kinds of voids: both atomistic and corresponding continuum results are reported in Fig. 3. Good agreement between atomistics and continuum is observed in any case. It is found that the crack creates the largest stress intensification; at variance, a cylindrical hole produces larger stress enhancement at far distances with respect to cracks of the same size.

We observe that stress atomistic data (see Fig. 3) are located at values x/r larger than 1; this is a consequence of the arbitrariness in defining the size r of the defects (as discussed in the previous section). As a result, although the stress enhancement of continuum elasticity is well reproduced by atomistic results, the limiting values for $x\rightarrow r$ are not actually reached by the atomistic data. This proves that the use of failure criteria based only on the maximum stress could be inadequate (a quantitative discussion of this issue is reported below). On the other side, the agreement between elasticity theory and present atomistic results stands for the possibility of using classical elastic solutions for the stress fields close to defects, even if nanosized and embedded in a discrete lattice.

At loads higher than the critical threshold $\sigma_A=\sigma_f$, a fracture originates from the defect and a brittle failure occurs along the (111) plane in all the considered cases (see Fig. 2 for the case of a system with a cylindrical hole). The results for a monocrystal containing a straight crack are reported in Fig. 4 as function of the crack semilength r. At vanishing r, the calculated critical stress approaches the ideal strength σ_{th} of the crystal. ASC and PSC curves, obtained by Eqs. (7) and (11) and by using l as fitting parameter, are reported in Fig. 4 as well. The two curves are almost identical and the atomistic data are well reproduced over all the investigated range. The fitted characteristic lengths for the two models are $l_{ASC}=6.0$ Å and $l_{PSC}=1.4$ Å. With respect to the previous estimate of λ, we get $l_{ASC}\sim\lambda$ and $l_{PSC}\sim\lambda/4$. The atomistic results have been compared also to the classical Griffith theory (dashed line in Fig. 4): they completely disagree in the region corresponding to small crack ($c\leqslant 20$ Å), where the Griffith curve diverges; good agreement is instead observed for large cracks. Furthermore, a representation of the atomistic data on a magnified vertical scale should emphasize a 10% deviation from the Griffith theory in the asymptotic limit of large cracks. This result was already observed by calculating the crack resistance as a function of the crack length, and it was attributed to lattice trapping effects.[20,27]

The calculated failure strength for a system with an infinite cylindrical hole is represented in Fig. 5 (open diamonds). The observed scattering of the atomistic data depends on the atomic-scale microstructure [see Fig. 2, panel (a)]. For hole radii $r\leqslant 20$ Å, a strong dependence of σ_f on the hole size is observed, while the elasticity prediction $\sigma_f/\sigma_{th}=1/3$ only represents the asymptotic limit for large radii. Both ASC (full line) and PSC (dot-dashed line) curves nicely reproduce the atomistic results, with better agreement found in the ASC case. The fitted lengths are in this case $l_{ASC}=6.6$ Å and $l_{PSC}=2.2$ Å, quite different values with respect to the expectations based on Eq. (1). Our calculations prove that the smallest cylindrical hole, corresponding to a missing row either of silicon or carbon atoms, reduces the ideal strength of the material by 18%. Furthermore, we performed the same calculations also on a pure silicon sample, obtaining a remarkably similar strength reduction of 18.5%.

For some hole radii (i.e., $r=5,10,15$ Å), we have computed the failure strength in plane stress border condition, by allowing the cell to relax in the x-y plane so as to obtain the conditions $\sigma_{xx}=0$ and $\sigma_{yy}=0$. The corresponding results are reported in Fig. 5 as cross symbols. It is apparent that our physical picture is not affected by border conditions.

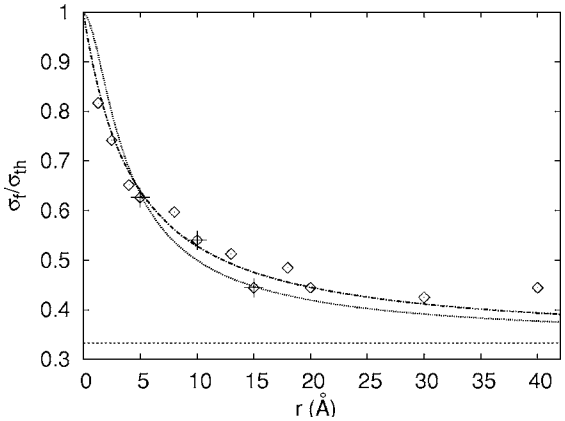

FIG. 5. Failure strength for a system containing a cylindrical hole. Diamond symbols represent the atomistic data in plane strain (symbols' thickness approximates the uncertainty in the definition of the cylinder radius, as explained in Fig. 2). Cross symbols represent the atomistic data in plane stress. The full and dot-dashed lines represent ASC and PSC data, respectively. The horizontal dashed line represents the linear elastic theory result $\sigma_f/\sigma_{th}=1/3$.

The results for the strength reduction due to a spherical hole are reported in Fig. 6. As for a cylindrical hole, σ_f strongly depends on the hole size. At variance of the previous cases, the agreement between PSC and atomistic data is not so good: the ASC works better over all the range of radii investigated. In particular, we have calculated for a single vacancy a 4% strength reduction: this result is nicely reproduced by ASC, while according to PSC a reduction less than 1% is expected. The best ASC and PSC fits were obtained by setting $l_{ASC}\sim 7.9$ Å and $l_{PSC}\sim 2.8$ Å, respectively; once again these values are quite different from the estimations provided by Eq. (1).

It is worth readdressing the above issue of failure strength reduction in the special case of a single missing row of atoms (a geometry corresponding to the smallest cylindrical hole). The very large reduction due to such small defect is not unusual at the nanoscale. Indeed, molecular mechanics calculations on carbon nanotubes[2,3] indicate that holes due to one- and two-atom vacancy defects could reduce failure strength by as much as ~26%. Such a prediction is further confirmed by recent QFM calculations.[11] Nevertheless, we understand that our results for failure strength reduction directly depend on both geometry (i.e., the crystallographic orientation of the defect) and loading conditions. Such dependence holds as well for similar fracture feature, such as, e.g., the lattice trapping, for which directional anisotropy is reported.[28]

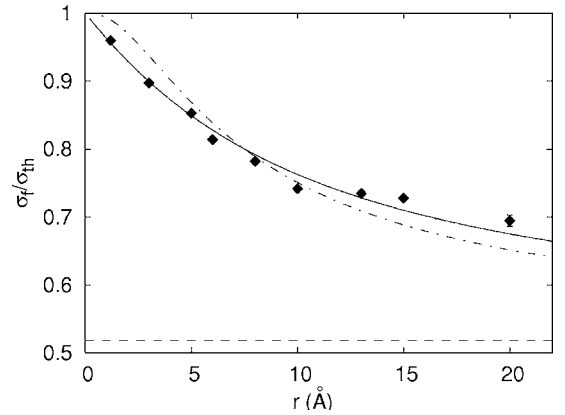

FIG. 6. Failure strength for spherical hole. Symbols represent atomistic data. The full and dot-dashed lines represent ASC and PSC data, respectively. The horizontal dashed line represents the linear elastic theory result $\sigma_f/\sigma_{th}=1/2$.

The present results seem to indicate that ASC works better than the PSC theory which, therefore, can be regarded just as an approximation of ASC. Furthermore, as already mentioned in Sec. I, the length scale l has not a clear interpretation within PSC formalism, while according to ASC it represents a meaningful estimation of the process zone size λ. Our simulation proves that λ is not a physical material parameter; rather, it is related to the defect geometry. In particular, it is found that the process zone is larger for holes than for cracks. A possible explanation is based on the existence of a larger flaw-tolerance regime for holes than for cracks. In fact, from Eqs. (7)–(9) we note that defects with size smaller than l are expected to slightly affect the failure stress (flaw-tolerance regime). At variance, if the size is larger than l, they are expected to dramatically affect the failure stress. Since the present calculations provide a stronger failure strength reduction for cracks than for holes of comparable dimensions, larger values for l are plausible for the latter (still considering the same material and structure).

By comparing the calculated length l_{ASC} with the interbond distance c_0 along the crack propagation direction, we obtain $l_{ASC}/c_0\sim 2$, 2, and 3 for the crack, the cylindrical hole, and the spherical hole, respectively. By looking at the process zone size as a unit for the discrete crack advancement (as suggested by ASC and QFM models), it turns out that the failure must proceed by finite steps as large as 2, 2, or 3 interbond distances for the above defects, respectively. Clearly, the assumption made by elasticity theory and LEFM for $\lambda\rightarrow 0$ would yield trivial results; on the other hand, we have shown that a process zone as large as few interbond distances can be introduced in order to reconcile continuum data to the atomistic picture.

V. CONCLUSIONS

By means of atomistic simulations, we investigated the effect on the failure strength of a $\beta-$SiC monocrystal induced by the presence of cracks, cylindrical holes, and spherical voids under uniaxial [111] loading condition. The atomistic results for small nanosized defects strongly deviate from those based on the elasticity theory; at variance, the elasticity nicely reproduces the atomistic data in the limit of large defects ($r>20$ Å). This result suggests that the process zone plays a fundamental role and cannot be neglected at least at the nanoscale. A validation of this conclusion is offered by the direct comparison between atomistics and the ASC theory, according to which the process zone size just represents a unit of discrete crack advancement. We provide an estimation for the process zone length by fitting ASC on present atomistic results. We also prove that such a charac-

teristic length actually depends on the defect type. Its value is estimated to be 0.60 nm for cracks, 0.66 nm for cylindrical holes, and 0.79 nm for spherical voids. The larger process zones associated with holes are interpreted as an evidence of a higher flaw-tolerance regime for holes and/or voids than for cracks.

ACKNOWLEDGMENTS

This work has been funded by MIUR under projects "PROMOMAT" and PON "CyberSar." We also acknowledge computational support by CASPUR (Rome, Italy) computing center.

*Corresponding author. Electronic address: luciano.colombo@dsf.unica.it

[1] L. J. Gibson and M. F. Ashby, *Cellular Solids: Structure and Properties* (Cambridge University Press, Cambridge, 1997).
[2] L. Mielke, D. Troya, S. Zhang, J. Li, S. Xiao, R. Car, R. S. Ruoff, G. C. Schatz, and Ted Belytschko, Chem. Phys. Lett. **390**, 413 (2004).
[3] S. Xiao and W. Hou, Phys. Rev. B **73**, 115406 (2006).
[4] G. R. Irwin, J. Appl. Mech. **E24**, 361 (1957).
[5] H. Neuber, *Theory of Notch Stress* (J. W. Edwards Brothers, Ann Arbor, MI, 1946).
[6] B. R. Lawn, *Fracture of Brittle Solids* (Cambridge University Press, Cambridge, 1975).
[7] K. B. Broberg, *Cracks and Fracture* (Academic, San Diego, 1999).
[8] A. A. Griffith, Philos. Trans. R. Soc. London, Ser. A **221**, 163 (1920).
[9] J. M. Whitney and R. J. Nuismer, J. Compos. Mater. **8**, 253 (1974).
[10] R. J. Nuismer and J. M. Whitney, ASTM Spec. Tech. Publ. **553**, 117 (1975).
[11] N. M. Pugno and R. S. Ruoff, Philos. Mag. **84**, 2829 (2004).
[12] N. M. Pugno, Int. J. Fract. **140**, 159 (2006).
[13] A. Carpinteri, *Mechanical Damage and Crack Growth in Concrete* (Martinus Nijhoff, Dordrecht, 1986).
[14] A. Catro-Montero, S. P. Shah, and R. A. Miller, J. Eng. Mech. **116**, 2463 (1990).
[15] B. L. Karihaloo, Eng. Fract. Mech. **35**, 637 (1990).
[16] V. M. Entov, Mech. Solids **11**, 105 (1976).
[17] V. Novozhilov, Prikl. Mat. Mekh. **33**, 212 (1969).
[18] F. Cleri, Phys. Rev. B **65**, 014107 (2002).
[19] J. Tersoff, Phys. Rev. B **39**, 5566 (1989).
[20] A. Mattoni, L. Colombo, and F. Cleri, Phys. Rev. Lett. **95**, 115501 (2005).
[21] M. Ippolito, A. Mattoni, L. Colombo, and F. Cleri, Appl. Phys. Lett. **87**, 141912 (2005).
[22] M. Ippolito, A. Mattoni, L. Colombo, and N. M. Pugno, Phys. Rev. B **73**, 104111 (2006).
[23] L. Landau and E. M. Lifshits, *Theory of Elasticity* (Butterworth-Heinemann, Oxford, 1986).
[24] M. Ippolito, G. Fugallo, A. Mattoni, L. Colombo, and F. Cleri, Strength, Fracture and Complexity **3**, 89 (2005).
[25] L. Colombo, M. Ippolito, A. Mattoni, and F. Cleri, in *Advances in Contact Mechanics: Implications for Materials Science, Engineering, and Biology*, edited by R. Buzio and U. Valbusa (Transworld Research Network, Kerala, India, 2006), p. 83.
[26] W. Li and T. Wang, Phys. Rev. B **59**, 3993 (1999).
[27] R. Thomson, C. Hsieh, and V. Rana, J. Appl. Phys. **42**, 3154 (1971).
[28] R. Perez and P. Gumbsch, Phys. Rev. Lett. **84**, 5347 (1999).